

**Mechanism Of Radical-Radical Reactions:
The Reaction Of Atomic Hydrogen With The Formyl Radical**

Lawrence B. Harding and Albert F. Wagner

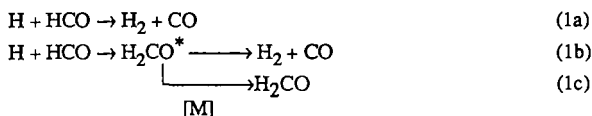
Chemistry Division, Argonne National Laboratory,
Argonne, IL 60439

Abstract

The addition and abstraction reaction pathways on the potential energy surface for H+HCO have been characterized by an *ab initio* four electron, complete active space, self-consistent field electronic structure calculation. The elimination pathway to go from the excited adduct H₂CO* to products H₂+CO has already been characterized by others[1]. All this information is used in variational transition state theory and RRKM calculations to calculate a rate constant as a function of temperature and pressure. The room temperature value agrees with the lowest of three experimental measurements. The results indicate that abstraction is the dominant process.

I. Introduction

While the dissociative dynamics of H₂CO have been well studied[1,2], the reverse reactions of the dissociation products are less well known. In particular the three measurements[3-5] of the rate of H+HCO differ by almost an order of magnitude and have only been done at room temperature. Like many radical-radical reactions, H+HCO has several possible pathways to reaction:



Reactions (1a) and (1b) are disproportionations by either direct, bimolecular abstraction or addition-elimination. Reaction (1c) is recombination by pressure stabilization of buffer gas [M]. In this theoretical study, the reaction pathway of abstraction (1a) and of adduct formation in (1b) and (1c) are characterized by electronic structure calculations. Then this information along with the characterization of the elimination of (1b) are used in dynamics calculations of the rate constant.

II. Potential Surface Calculations

The calculations reported here employ the Dunning[6], valence, double-zeta contractions of the

*Work performed under the auspices of the Office of Basic Energy Sciences, Division of Chemical Sciences, U. S. Department of Energy, under Contract W-31-109-Eng-38.

Huzinaga[7] (9s,5p) sets of oxygen and carbon centered primitive Gaussians. For the hydrogens the (4s/2s) contraction was used with a scale factor of 1.2. In addition sets of d polarization functions were centered on the carbon and oxygen ($\alpha_C=0.75$, $\alpha_O=0.85$) and one set of p polarization functions on each of the hydrogens ($\alpha=1.0$).

With this basis set, four electron, four orbital complete active space, self-consistent field (CASSCF) calculations were carried out. In this wavefunction the four electrons involved in the two CH bonds of formaldehyde are correlated with all possible orbital occupations of four orbitals, a total of 20 configurations. The remaining electrons are not correlated. With the exception of minor differences in the basis set, this is the same wavefunction used by Dupuis et al[1].

The calculations were carried out with the Argonne QUEST-164[8] programs, SOINTS and UEXP. An average calculation on a planar point took approximately 11 minutes on the FPS-164 while a typical nonplanar point required 16 minutes. The energy was evaluated at a total of approximately 300 points.

Initially it was assumed that the addition and abstraction reaction coordinates could be approximated by the distance between the carbon and the incoming hydrogen. The grids of points were calculated at 0.5 au increments in this CH distance along the two paths. A total range of CH distances from 5 to 10 au was covered. Variations in the inactive geometrical parameters of 0.05 au for bond lengths, 5°-10° for bond angles and 10°-20° for the dihedral angle were used. These grids of points were then fit separately to Simons-Parr-Finlan type expansions, using the program SURVIB[9], in order to obtain local representations of the potential surface in the region of the abstraction and addition reaction paths. The dependence of the energy on the angle of approach is depicted in Figure 1. From this figure it can be seen that there are two distinct reactive channels, one corresponding to abstraction and one to addition. The calculations predict no significant barrier in either channel.

The two reaction paths were then obtained by following steepest descent paths in mass-weighted, atomic cartesian coordinates. The starting points for the two paths were obtained by freezing the CH distance at 8 au and optimizing the remaining geometrical parameters. Two minima were found in this procedure (see Figure 1), one in which the incoming hydrogen is trans to the HCO hydrogen and a second in which the two hydrogens are cis, these were used as starting points for the addition and abstraction paths respectively. A plot of the energy along the two reaction paths is given in Figure 2. Vibrational frequencies were obtained along the reaction paths by numerically calculating the second derivative matrix in mass-weighted atomic cartesian coordinates, projecting out the translations, rotations, and gradient vector, and then diagonalizing the resulting 5 dimensional matrix. Plots of the vibrational frequencies along the two reaction paths are given in Figures 3 and 4.

III. Rate Constant Calculations

The calculated frequencies, structures and energetics as a function of distance along the reaction path can be used directly in a variational transition state theory (VTST) calculation to produce the abstraction rate constant, i.e., for Reaction (1a). In this calculation, the rate constant at each temperature is that one which is a minimum with respect to position along the reaction path. Two of

the vibrational frequencies go to free rotations of the HCO in the reactant asymptote. The partition function used in the VTST expression for these two degrees of freedom is approximated as the minimum of the vibration or free rotation partition function. Subsequent calculations will include the hindered rotor effects. The resulting abstraction rate constant is shown in Fig. 5 along with the three rate constants measurements referred to in the introduction.

The measurements include both abstraction and addition processes. The VTST rate constant for addition is also in Fig. 5. This rate constant was determined in the same way as for abstraction, only with the calculated addition frequencies, structures and energetics. However, unlike abstraction, this rate constant can not be directly compared to experiment because it is only an adduct formation rate constant to form metastable, highly vibrationally excited H_2CO^* . H_2CO^* may decay back to reactants, may go on to products by eliminating H_2 , i.e., Reaction (1b), or may be stabilized by buffer gas to thermalized H_2CO , i.e., Reaction (1c). That fraction of the adduct formation rate constant that corresponds to elimination or stabilization is what is needed for comparison to experiment. To determine that fraction, characterizations of the potential energy surface in the region of the H_2CO equilibrium and the elimination transition state $\text{H}\cdots\text{H}\cdots\text{CO}$ are required. Then the stabilization rate constant and variational RRKM theory can be used to calculate the rate constant for Reactions (1b) and (1c).

In electronic structure calculations of comparable quality, Dupuis et al.[1] characterized the structure and frequencies of both H_2CO at equilibrium and the $\text{H}\cdots\text{H}\cdots\text{CO}$ elimination transition state. The calculated properties at the equilibrium are very close to the experimental values and for consistency are used in the rate constant calculations. In a careful study of the energetics, the best estimate of the calculated barrier height to elimination is 81 ± 3 kcal/mole with the zero point energy correction. Experimental values[2] for the energetics give a number of about 84 ± 1 kcal/mole. The experimental value for the energetics of H_2CO dissociation to $\text{H}+\text{HCO}$ is about 86 ± 2 kcal/mole and is due to thermochemical measurements with the uncertainty from the heat of formation of HCO[10]. These experimental values for the energetic placement of asymptotes and barrier heights will be used in the rate constant calculations.

With the transition states selected at each temperature by the VTST calculation for formation of the adduct, chemically activated RRKM calculations were performed to determine the subsequent fate of the adduct. These calculations are of a standard form[11] with total angular momentum approximately included only as a thermally averaged value. A direct count Beyer-Swinehart algorithm[12] is used. Tunneling through the elimination barrier is included in an Eckhart manner[13]. The final pressure dependent rate constant produced is in the high pressure limit the adduct formation rate constant in Fig. 5.

The calculations require as input the rate constant for stabilization of the H_2CO^* by buffer gas. In the three experiments, the buffer gas differs. CO, H_2CO , and Ar were used at pressures ranging from a few torr to atmospheric. Under these conditions, stabilization of the adduct turns out to be an unlikely event and the calculations are not particularly sensitive to detailed specifications of the stabilization rate constant. The rate constant used is the the Lennard-Jones gas kinetic rate constant

times an efficiency factor for stabilization. The Lennard-Jones parameters are taken from the tabulation of Ref. 14 with the values for ethylene used for H_2CO^* . The efficiency factor is determined in a way to empirically mimic a master equation solution[15] and requires as input the average energy $\langle\Delta E\rangle$ transferred between buffer gas and metastable adduct per up and down collision. This value used (-20 cm^{-1}) were those measured[16] for CS_2 , the only triatomic where direct measurement of $\langle\Delta E\rangle$ have been published. $\langle\Delta E\rangle$ was presumed to be independent of temperature[17].

To complete the input for the chemically activated RRKM calculations, the external rotations of the equilibrium and saddle points must be classified as either active or adiabatic. The external rotations are presumed similar to those of a symmetric top. The conserved total angular momentum and its projection on a space fixed axis are associated with the two larger moments of inertia and are treated adiabatically. The projection of the total angular momentum on the molecular axis is associated with the smallest moment of inertia and is not necessarily a conserved quantity. If there is substantial vibration-rotation interaction through centrifugal stretching or Coriolis coupling, the energy associated with this projection becomes active[18]. The amount of vibration-rotation interaction in $\text{H}+\text{HCO}$ is unknown and so in the calculations this degree of freedom was treated both ways, either actively or adiabatically. Fortunately the results are not particularly sensitive to the choice and only those for the active treatment will be discussed.

In Fig. 5 the final calculated rate constant for reactions (1b) and (1c) as a function of pressure in Ar buffer gas is displayed for two different choices of the energetics of dissociation of formaldehyde. As mentioned above the experimental uncertainties in both the height of the elimination barrier and the $\text{H}+\text{HCO}$ asymptote relative to the bottom of the H_2CO well are a few kcal/mole. The two cases in Fig. 5 are for the difference between the asymptote and barrier (i.e., ΔE) being as large or as small as these uncertainties allow. The pressure dependence of the calculated rate constants show that stabilization (1c) is a minor process relative to elimination (1b) although, as expected, it is more important if the elimination barrier and the $\text{H}+\text{HCO}$ asymptote are very close to one another. The importance of elimination should increase with changing the buffer gas to CO or H_2CO but not so as to qualitatively change the results. The figure also shows by comparison to the adduct formation rate that the most likely fate of the adduct is to decompose back to reactants. This is due to the fact that the elimination transition state is a tight, constricted configuration and the lifetime of the adduct (which controls stabilization) is short because it is only a 4 atom system. As a result, direct abstraction is the dominant process. The sum of abstraction, addition-elimination, and stabilization rate constants gives a total rate constant at or slightly below (depending on the choice of energetics) the lowest and most recent experimental value[5].

References

1. M. Dupuis, W. A. Lester, Jr., B. H. Lengsfeld III and B. Liu, *J. Chem. Phys.* **79**, 6167 (1983) and references therein.
2. C. B. Moore, *Ann. Rev. Phys. Chem.* **34**, 525 (1983).
3. J. P. Reilly, J. H. Clark, C. B. Moore and G. C. Pimentel, *J. Chem. Phys.* **69**, 4381 (1978).
4. V. A. Nadochenko, O. M. Sarkisov and V. I. Vedeneev, *Dokl. Akad. Nauk SSSR*. **244**, 152 (1979).
5. C. J. Hochenadel, T. J. Sworski and P. J. Ogren, *J. Phys. Chem.* **84**, 231 (1980).
6. T. H. Dunning Jr., and P. J. Hay, "Methods of Electronic Structure Theory", H. F. Schaefer III, Ed., Plenum Press, New York, 1971, Chapter 1.
7. S. Huzinaga, "Approximate Atomic Wavefunctions. I", Chemistry Report, University of Alberta, Edmonton, Alberta, Canada, 1971.
8. R. Shepard, R. A. Bair, R. A. Eades, A. F. Wagner, M. J. Davis, L. B. Harding, T. H. Dunning Jr., *Int. J. Quantum Chem. Symp.* **1983**, 17,613.
9. L. B. Harding and W. C. Ermler, *J. Comp. Chem.* **1985**, 6,13.
10. P. Warneck, *Z. Naturforsch. Teil A* **29**, 350 (1974).
11. P. J. Robinson and K. A. Holbrook, *Unimolecular Reactions* (Wiley-Interscience, New York, 1972) Chaps. 4 and 8.
12. D. C. Asholtz, J. Troe and W. Wieters *J. Chem. Phys.* **70**, 5107 (1979).
13. W. H. Miller, *J. Amer. Chem. Soc.* **101**, 6810 (1979).
14. H. Hippler, J. Troe and H. J. Wendelken *J. Chem. Phys.* **78**, 6709 (1983).
15. J. Troe, *J. Phys. Chem.* **1983**, 87, 1800.
16. J. E. Dove, H. Hippler and J. Troe *J. Chem. Phys.* **82**, 1907 (1985).
17. M. Heymann, H. Hippler and J. Troe *J. Chem. Phys.* **80**, 1853 (1984).
18. W. Forst, *Theory of Unimolecular Reactions* (Academic Press, New York, 1973) Chap. 5.

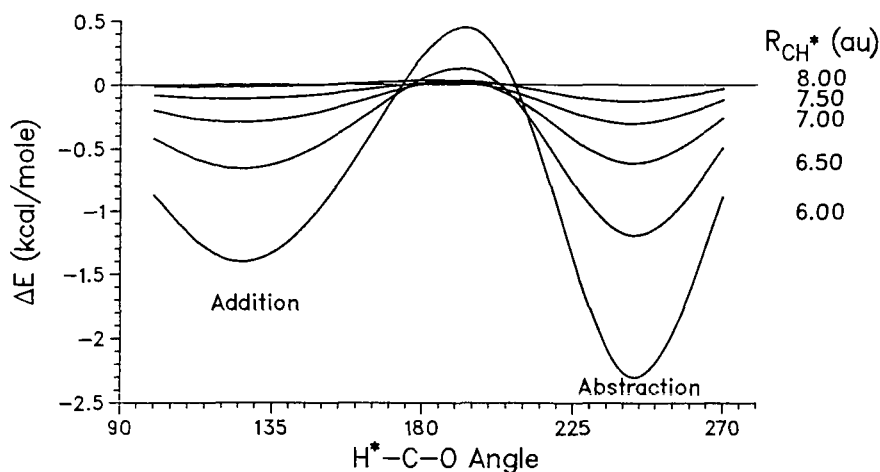


Figure 1. Angular dependence of the energy in the approach of atomic hydrogen to the formyl radical.

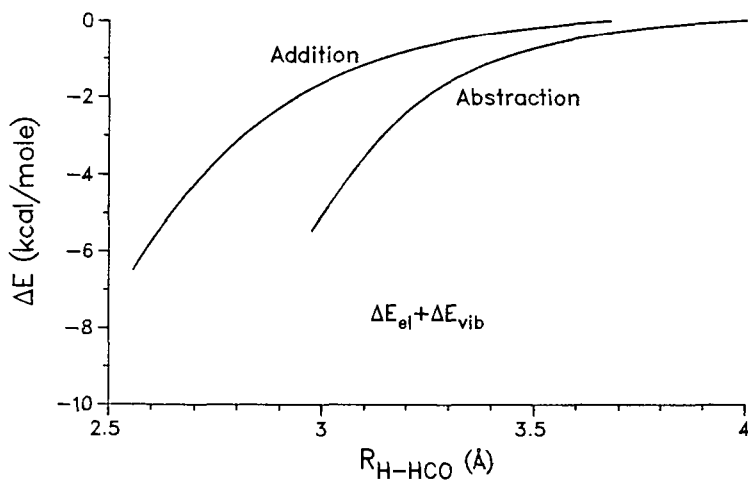


Figure 2. Energy profiles along the addition and abstraction reaction paths.

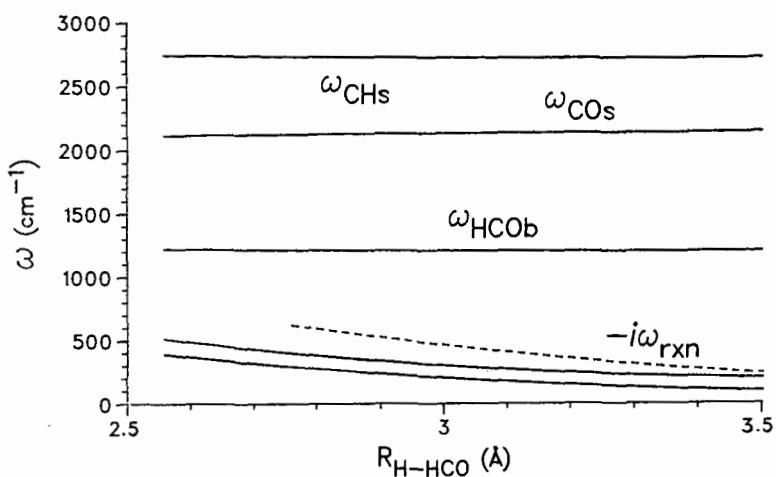


Figure 3. Vibrational frequencies along the addition reaction path.

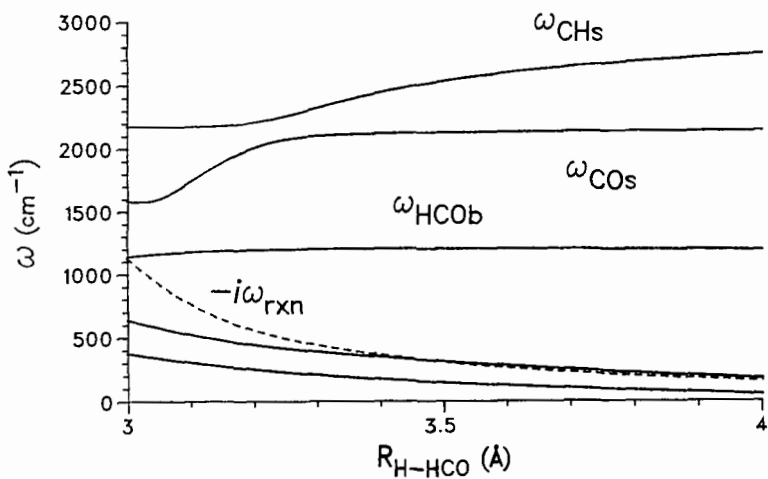


Figure 4. Vibrational frequencies along the abstraction reaction path.

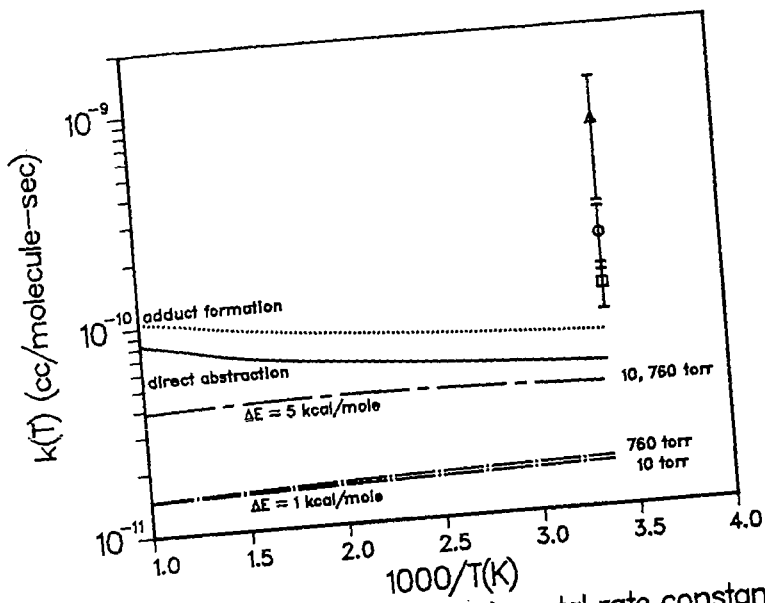


Figure 5. Calculated and experimental rate constants versus inverse temperature